

Fluid flow dynamics in deformed carbon nanotubes with unaffected cross section

Mohammad Rezaee, Arian Yeganegi, Mohammad Namvarpour and Hojat Ghassemi*

School of Mechanical Engineering, Iran University of Science & Technology, Narmak, Tehran, Iran

(Received January 18, 2021, Revised October 12, 2021, Accepted October 13, 2021)

Abstract. Numerical modelling of an integrated Carbon NanoTube (CNT) membrane is only achievable if probable deformations and realistic alterations from a perfect CNT membrane are taken into account. Considering the possible forms of CNTs, bending is one of the most probable deformations in these high aspect ratio nanostructures. Hence, investigation of effect associated with bent CNTs are of great interest. In the present study, molecular dynamics simulation is utilized to investigate fluid flow dynamics in deformed CNT membranes, specifically when the tube cross section is not affected. Bending in armchair (5,5) CNT was simulated using Tersoff potential, prior to flow rate investigation. Also, to study effect of inclined entry of the CNT to the membrane wall, argon flow through generated inclined CNT membranes is examined. The results show significant variation in both cases, which can be interpreted as counter-intuitive, since the cross section of the CNT was not deformed in either case. The distribution of fluid-fluid and fluid-wall interaction potential is investigated to explain the anomalous behavior of the flow rate versus bending angle.

Keywords: carbon nanotube; desalination graphene; flow rate; monatomic fluids

1. Introduction

Researchers have placed a spotlight on CNTs since their discovery by Iijima in 1991 (Iijima 1991), performing numerous studies on the nanostructure and its properties. CNTs have many remarkable properties such as semi-conductivity, superior mechanical stability and elastic properties under high strain and load, making these structures one of the most exciting materials (Chu *et al.* 2015).

In consideration of their extraordinary properties, various applications for these nanostructures, such as the use of CNTs to boost water desalination (McGinnis *et al.* 2018), drug delivery (Panwar *et al.* 2019, Madani *et al.* 2011), air filtration (Yildiz and Bradford 2013, Li *et al.* 2014, Zhang and Wei 2019), bio sensing (Wang *et al.* 2006, Narang 2019), supercapacitors (Wu *et al.* 2017) and even petroleum filtration (Arash and Wang 2014) are proposed. Investigating the efficacy of many such applications requires comprehension of molecular-scale governing principles. To clarify ambiguous experimental findings and numerical results, it is important to understand the molecular mechanisms on this scale.

Molecular dynamics simulations are widely used as a numerical tool to understand the principles and explore nanoscale unclear areas, particularly, the unique transport behavior of nanoconfined fluids. Important researches have been carried out, using molecular dynamics, to analyze flow dynamics in the CNTs (Majumder *et al.* 2005, Hummer *et al.* 2001, Pérez-Sánchez 2017, Köhler *et al.* 2019, Cao *et al.*

2006, Liakopoulos *et al.* 2016, 2017). Particularly, while deformation of carbon nanotubes under synthesis and membrane manufacturing processes (Li *et al.* 2012) is unavoidable and has been verified by experimental observation (Barzegar *et al.* 2017, Yuan *et al.* 2012), its associated effects on transport behaviour of various types of fluid is studied in the literature. Transport diffusion of helium gas across deformed CNTs was examined by Feng *et al.* (2018). In their work, effect of temperature was investigated, and it was shown that variations in the cross section of the tube contributed to a substantial reduction in the rate of helium flow rate. Furthermore, a study of particle transport in graphene membrane nano-pores, using non-equilibrium molecular dynamics, was conducted by Wen *et al.* (2015). Their goal was to find out the impact of pore shape and form on diffusion of gas particles. The results of their work, revealed that circular pore leads to the maximum flow rate, and dissymmetry in pore cross section would cause a reduction in gas flow rate. Lu *et al.* (2008) studied effects of nanochannels deformations on the gating of water permeation and the pattern of the density distribution of water inside the channel. Their findings showed that, in relation to the channel deformation, the behavior of the changes in wavelike water density distributions is found to correlate with the gating of the water permeation. Razmkhah *et al.* (2017), investigated the effects of CNT shape on the capacity of desalination, through MD simulation. Using three different shapes of nanotubes, they found that unlike tubular CNT, cone CNT was always full and water molecules passed through it continuously, therefore, higher flow rate was obtained. However, the amount of salt rejection in deformed cases were slightly decreased. In other words, they showed that the entrance of CNT has an impact on the amount of salt

*Corresponding author, Ph.D.,
E-mail: h_ghassemi@iust.ac.ir

rejection as well as the water conductance. Zhou *et al.* (2013), examines the influence of deformation of CNTs on water flux and the pumping capacity. Consequently, in the research, it is found out that deformation has a major role in pumping water molecules across CNT, and surprisingly at a certain deformation depth, in fact, an increase in water flux is recorded. In addition, effect of elliptical cross section on transportation of water molecules through CNTs was investigated by Robinson *et al.* (2019). Results indicated that flow rate of water is noticeably dependent on deformations of cross section. Mendonca *et al.* (2018, 2020) conducted a meticulous study on relationship of water flow rate with eccentricity of the elliptical CNT. Analyzing behavior of water inside nanotubes with and without deformation, they observed alterations in flow rate that were not monotonic, also, they found that generally, perfect nanotubes result in a greater diffusion than deformed nanotubes. He *et al.* (2012) studied how a narrow region along a perfect CNT would affect water flow rate. The results illustrated that depending on the position of deformation, a significant reduction occurs.

In most of the researches on effects of CNT deformations, cross section of the tube is considered to be changed due to deformation, hence flow rate showed strong dependency and variations. Meanwhile, some probable forms of non-ideal CNTs in a membrane does not involve meaningful changes in the cross section (Shima 2012). The interest here lies in studying effects associated with deformed CNT membranes with perfect cross sections, which are not studied in the literature. On the other hand, simulation of monoatomic fluids flow is remarkably useful in inference of descriptive models for atomic structure and fluid dynamics in narrow CNTs. The general model utilized to describe monoatomic interactions, allows for extending the conclusions to a wide variety of liquids of more complex structures. On the other hand, less complexity assigned with argon in comparison to water, approves the researchers to reduce the analysis and search for more fundamental insights. In this study, flow rate of monoatomic fluid through alternative forms of CNT membranes is investigated. Furthermore, microscopic parameters of fluid-wall interaction potential and atomic axial velocity are studied to inspect the effects of deformation.

2. Methodology

Initially, bent CNTs with chirality of (5,5) were generated by exerting pushing forces in x direction on a perfect CNT. The external forces acting on the CNT were defined as a function of CNT transverse deflection in order to achieve the desired bending in each case (Fig. 1). The carbon-carbon interaction is modelled by Tersoff potential (Tersoff 1988) with the parameters adopted from Brenner (Brenner 1990).

Once the bent CNT is ready, flow rate of argon atoms through them is investigated using numerical simulations. To have a simulation for argon atoms flow rate in LAMMPS, a system was assembled which included four graphene sheets and a bent CNT.

On the next step, inclined CNTs were formed by the

Table 1 Model parameters used in argon flow simulation (Ackerman *et al.* 2003, Kaukonen *et al.* 2012, Rezaee and Ghassemi 2020)

Interaction	Well depth of potential, ϵ (J)	LJ distance at zero inter-atomic potential, σ (m)	Mass (kg)
Ar-Ar	1.71e-21	3.42e-10	6.633e-26
Ar-C	9.08e-22	3.48e-10	-
C-C	No interaction		1.994e-26

means of rotating the original vertical CNT about its center point to reach a specific desired angle.

Subsequent to the formation of inclined CNT and determination of the simulation domain, molecular dynamics (MD) simulations were implemented in LAMMPS to study argon atoms flow rate. The inclined CNT was placed between two graphene sheets functioning as membrane walls, also, two more graphene sheets were used which served as pistons to contain and restrict the argon atoms. The graphene sheets are considered 5.0 nm in 5.0 nm, unless otherwise declared. In addition, the boundary conditions for both x and y directions were set to periodic so as to avoid results of geometrical constraints.

The total number of argon atoms exceeds 9500, high enough to avoid interaction between the piston wall and the membrane wall. These atoms are split equally between the two reservoirs in the beginning. The well-known Lennard-Jones potential is implemented to model interactions between the atoms with the parameters as illustrated in Table 1.

According to literature, it is well-understood that application of realized numerical configurations is of vital importance in molecular dynamics simulations in order to have valid conclusions (Ritos *et al.* 2015). There are different ways for applying pressure gradient to a system (Cannon and Hess 2010, Barclay and Lukes 2016, Derakhshan *et al.* 2015, Huang *et al.* 2006, Docherty *et al.* 2014). The appropriate method should have two main characteristics: first, causing the argon atoms to flow through the pore and secondly, rejecting backflow (Rezaee and Ghassemi 2020). Moreover, it is essential that the effects of pressure gradient on the flow rate of argon be unambiguous. In order to achieve that, a variable force was exerted on the graphene sheets at the two ends, which is calculated as sum of two terms:

$$f_{j,z} = f_{ext} + f_{avg-fp} \quad (1)$$

Here, $f_{j,z}$ is the total force to be exerted on atom j in z direction, and f_{avg-fp} is the average force of all fluid-piston pairwise interaction force given by:

$$f_{avg-fp} = \frac{\sum_{i=1}^{N_{fluid}} \sum_{j=1}^{N_{piston}} F_{i,j}}{N_{piston}} \quad (2)$$

and f_{ext} , which is proportional to the desired pressure of the reservoir, is the external force exerted on piston atoms:

$$f_{ext} = \frac{P.A}{N_{piston}} \quad (3)$$

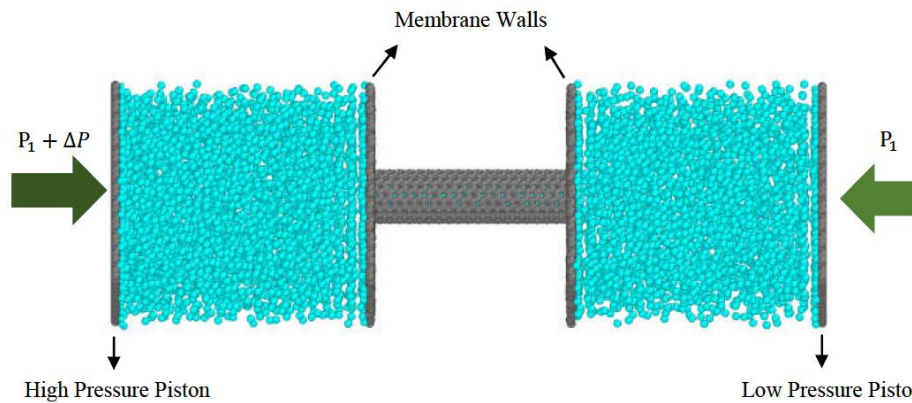


Fig. 1 The simulation domain. The open source software Ovito (Stukowski 2010) was used to render the image

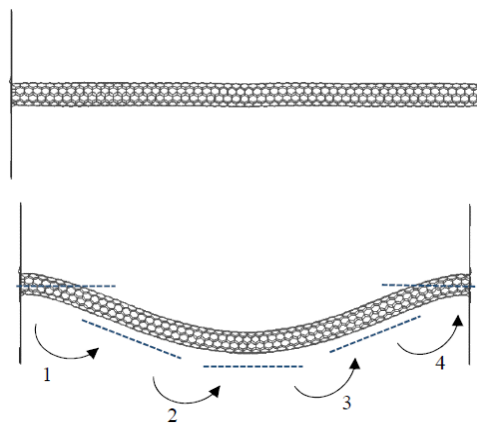


Fig. 2 Straight and bent CNTs with uniform cross sections in a membrane

in which P and A indicate absolute pressure and total area of the membrane, respectively. Also, the piston atoms are limited to move merely in z -direction, therefore, the structure of the pistons will maintain rigidity along the simulation. Fig. 1 shows the geometry of the domain. In order to ensure rapid diffusion and slight sampling error, the pressure difference is set as high as 1000 bar.

Based upon literature, in this simulation the carbon-carbon interaction in inclined CNT and graphene sheets is neglected (Alexiadis and Kassinos 2008, Ang *et al.* 2019, Chen *et al.* 2008, Zhou *et al.* 2013, Shen *et al.* 2016). As a result, the tube walls are considered a fixed structure, nevertheless, by using a Nosé-Hoover thermostat (Nosé 1984, Hoover 1985), a simple spring model was applied on membrane walls to sustain the system temperature at 100 K. Whereas, no thermostat is applied on argon atoms (Alexiadis and Kassinos 2008, Ang *et al.* 2019). This consideration is exceptionally important to avoid non-physical changes in fluid atoms movement, especially in nanoscale confined flow (Kannam *et al.* 2013, Wang *et al.* 2017, Suga *et al.* 2018).

In the start of the simulation, two fixed mathematical bouncy walls for fluid atoms were used in both sides of the CNT, confining the fluid atoms in the reservoirs and restricting them from entering the CNT. These bouncy walls will exist only until temperature equilibrium is reached in both reservoirs. Time-step is set to 1 fs and in most cases equilibrium is reached in 10^6 steps (1 ns). The

flow rate data obtained from simulation is gathered for at least 100 ns after equilibrium is reached. The final average value of flow rate, attained in every case, was converged to a constant value with fluctuations only within 1 percent of that value. Also, in a previous study (Rezaee and Ghassemi 2020), different methods for ensuring the consistency of the model was implemented including, radial distribution function and effects of CNT length and pressure difference on flow rate results.

The flow rate data were gathered for at least 100 ns afterward. In every case, the average flow rate was converged to a constant value with no additional changes more than 1 percent of the value. Moreover, consistency of the model was previously (Rezaee and Ghassemi 2020) checked with several methods such as radial distribution function and effects of CNT length and pressure difference on flow rate results.

3. Results and discussion

In order to assess the effect of bending on the flow rate of argon through CNTs, at first, the flow rates of a straight nanotube, with the length of 13.63 nm and diameter of 6.78 Angstroms, and the bent form of the same tube were compared. The bending doesn't affect the cross section at any point, and the cross section remains a constant circle throughout the bent CNT. This point is clearly illustrated in

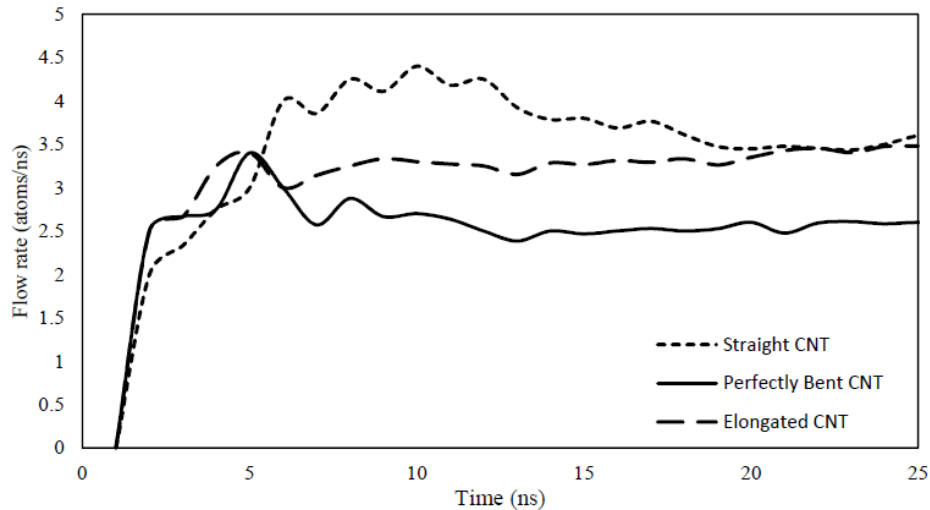


Fig. 3 Convergence trend and flow rate values in three cases of straight, bent and elongated CNTs



Fig. 4 Simplified bend in a nanotube

Fig. 2. This study was merely conducted to show that flow rate is not affected by bending in tubes, which seems plausible at first sight. In other words, it was assumed that since there are no significant changes in the cross section of the tube, the flow rate shouldn't fluctuate due to the bending. In spite of this, the results presented in Fig. 3 illustrate that bending causes the flow rate to decrease noticeably, around 30 percent.

Considering the process of deforming the CNT and obtaining a bent one, during which the two graphene sheets on the sides of the CNT were fixed, it seems natural that the CNT has elongated. Also, from previous researches, it has been observed that elongation of CNTs can result in a reduction in flow rate. Therefore, another simulation was conducted on a straight CNT, which was subjected to an appropriate tensile force to reach the same length as the bent CNT investigated previously. Results gathered from this case indicate that, although there has been a reduction in flow rate, the magnitude of the decrease is not even close to the bent CNT. Flow rate and convergence process are illustrated for each case in Fig. 3. Therefore, it can be concluded that the considerable reduction in flow rate through bent CNT, can't be merely an effect of elongation and despite the expectations, the bending alone has negative effects on the flow rate, even when cross section is uniform.

Subsequently, due to the clear result that flow rate is in

fact affected by bending of CNTs, it is essential to investigate simpler structures in order to quantify the bent effect, solely. As it is clearly illustrated in Fig. 2, the primary bent CNT includes four bends of which at least two are different in terms of angle and curvature radius. Hence, the results of numerical simulations are affected by a combination of these factors, therefore, it's impossible to investigate and quantify the direct effect of a single bent. Some simplifications must be implemented in order to resolve this issue. For this reason, a new system, illustrated in Fig. 4, was considered. This system is constituted of a simple bend with a specific angle and curvature radius. Nevertheless, this system, also, can't be considered as a completely simplified case since the axes of CNT aren't perpendicular to the graphene sheets at the two ends. In other words, the cross section of the entrance and exit of CNT are elliptic. Besides that, the inclined axis of nanotube near the membrane walls influences fluid-fluid interaction potential. To make sure of this effect, simulation of inclined CNT with different entrance angles were studied separately.

As it is illustrated in Fig. 5 besides the perpendicular CNT, argon flow rate in inclined CNTs with rotation angles of 15, 30, 45, and 60 degrees were studied. Results of this study are presented in Fig. 6. As it is clearly shown in the figure, with constant length and diameter, the angle of CNT inclination, in other words the angle between CNT axis at

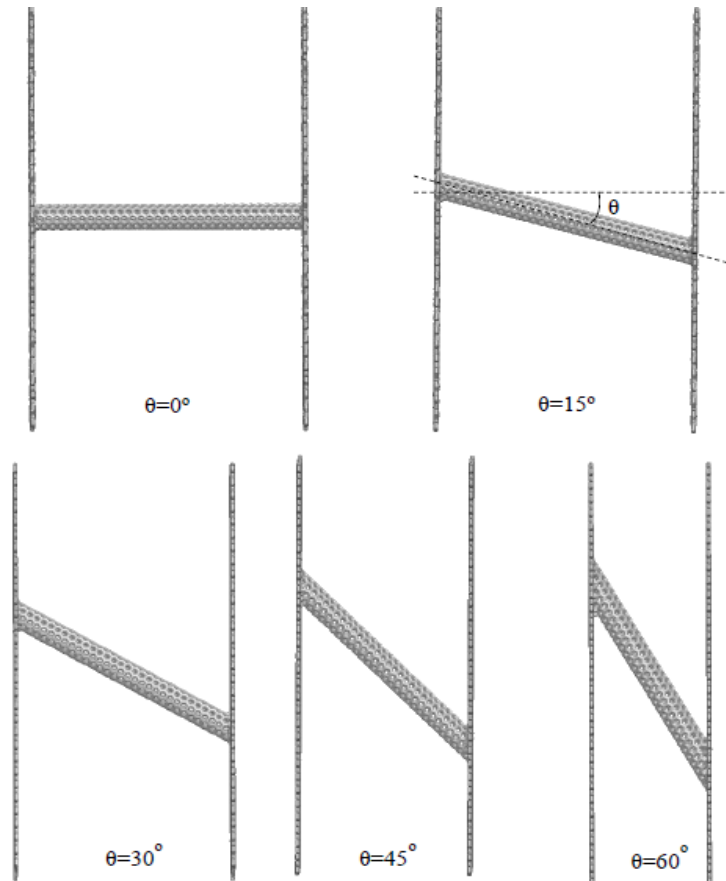


Fig. 5 Investigating the effect of entrance angle on flow rate

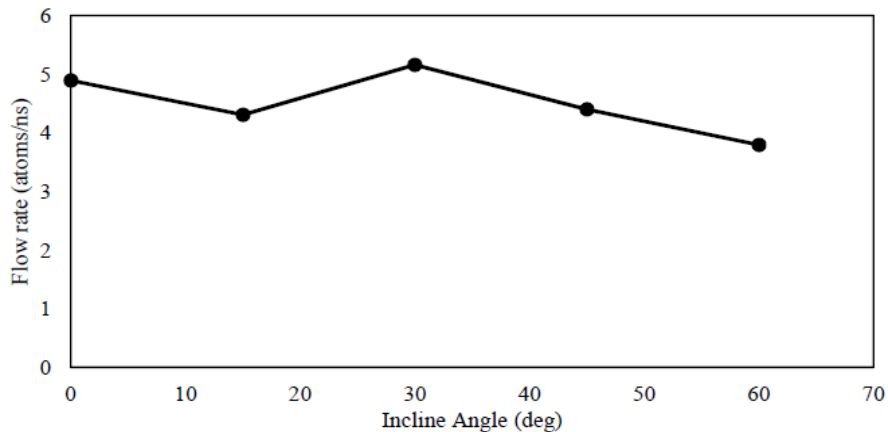


Fig. 6 Effect of inclination angle on the flow rate

entrance and graphene sheet, has a noticeable impact on fluid flow rate. This impact, which can be as great as 20 percent of the value, is not monotonic. Fig. 7 illustrates the fluid-fluid potential distribution experienced by the fluid particles passing through the entrance of nanotube. This figure proves the considerable effect of inclination of the path, separately and apart from the effect of elliptic entrance of nanotube.

Asserting the noticeable effect of CNT inlet angle on the flow rate, it has been shown that considering Fig. 4 as an illustration of the problem will not lead to an accurate and precise study on the pure effect of nanotube's bending.

Another significant factor influencing the flow rate is also introduced in the above-mentioned scenario. Conditions must, therefore, be provided so that the nanotube is perpendicular to the surface of the membrane, while maintaining its bending. The system was produced as shown in Fig. 8 to aim for such conditions. In this case, between two diagonal membranes, a bent nanotube is enclosed in a way that both membranes create right angles with nanotube inlets. The length of the membranes is increased so that the entire domain can be contained, which does not have a substantial effect on the results of our study. Systems were created in various bent angles and the argon

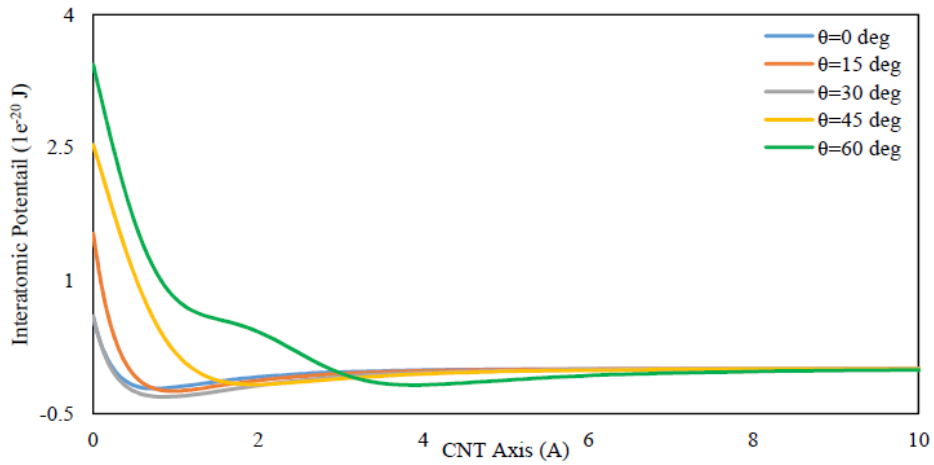


Fig. 7 Fluid-fluid potential distribution experienced by the fluid particles inside nanotube and upstream reservoir along the CNT axis

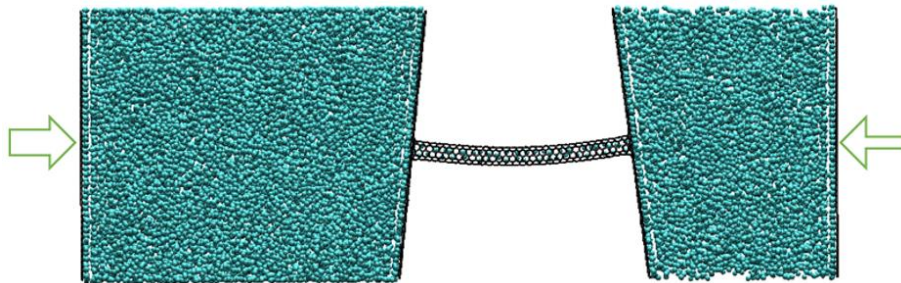


Fig. 8 Analyzing the flow rate in the bent nanotube, without putting the effect of inlet angle into consideration

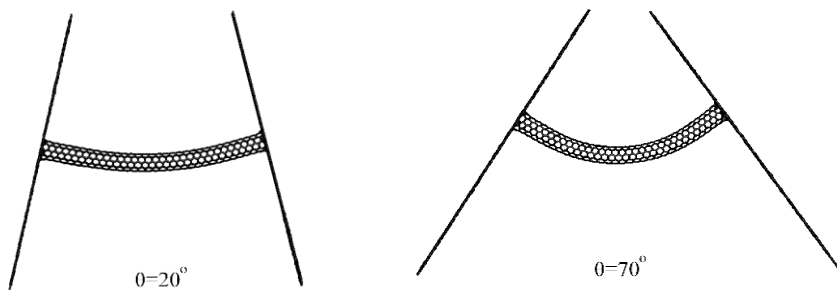


Fig. 9 Analyzing the flow rate in the bent nanotube, without putting the effect of inlet angle into consideration, 2 sample angles

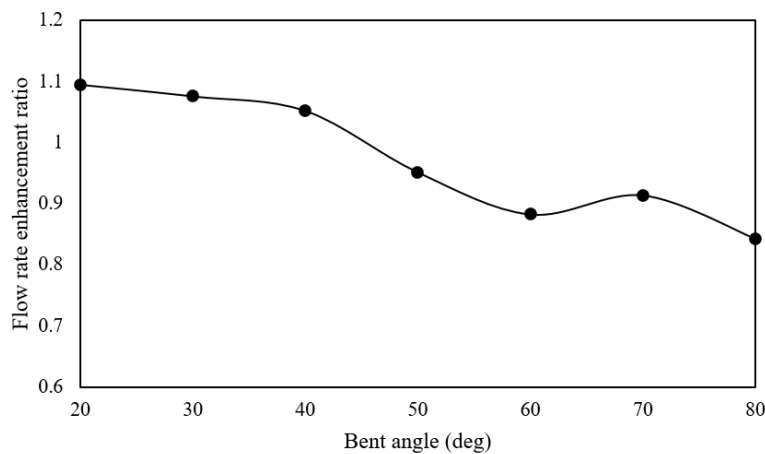


Fig. 10 Flow rate enhancement versus bent angle

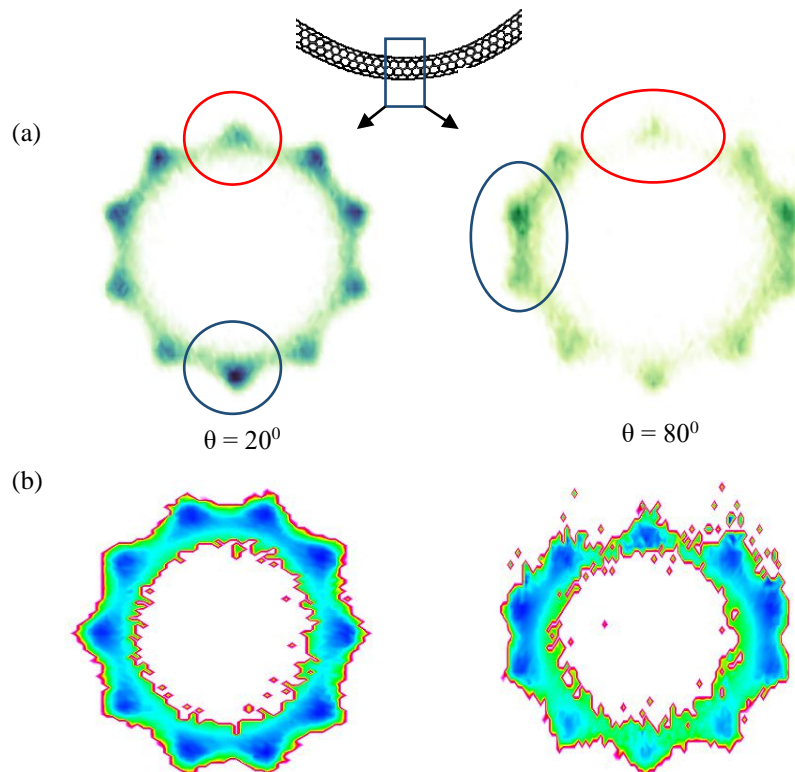


Fig. 11(a) The average distribution of fluid atoms in the cross section of bent CNTs, and (b) the distribution of the fluid-solid interaction potential in the same two cases

flow within them was studied. In Fig. 9, two such structures are illustrated. As shown in Fig. 10, the results showed that the flow rate decreases as the bent angle increases. A more detailed look on the cross section of the bent tube, may explain this behaviour. Fig. 11(a) shows that the distribution of atoms passing through CNT is significantly affected in bent cases. As seen in this figure, the fluid atoms tend to avoid the inner curvature. This effect can be significant in changing the atoms path through CNT, and decreasing the flow rate value. On the other hand, the distribution of fluid-solid interaction potential also appears to be non-uniform in bent CNT, while it depends only on wall parameters and is symmetrical in straight nanotubes (Sofos *et al.* 2016). Fig. 11 (b) shows this distribution for two cases of bent angles ($\theta = 20$ and $\theta = 80$). When compared to straight CNT, the variation of fluid-solid interaction, which is experienced by the fluid atoms, increases the resistance against the fluid flow, leading to lower flow rate in cases with higher bent angles. The effect is substantial in the region near the compressed CNT perimeter, which is the inner part of the bending curve (upper region in Fig. 11).

4. Conclusions

Effects of different deformations and alterations in CNT membranes on the flow of monoatomic fluid is investigated. MD simulation was carried out to model the CNT deformation, having Tersoff potential describing carbon-carbon bonded interaction. Afterwards, the argon flow was modeled in a long enough simulation to obtain the flow rate

variations in deformed cases. Armchair CNTs of (5,5) were considered. At first, the effect of CNT bending on the flow rate is proven to be significant, using simulation of a complex bent CNT structure. Then it was shown that angle of entry for CNT to the graphene membrane is an effective parameter. The average fluid-fluid interatomic potential function along the CNT axis in each inclined case justified the non-monotonic behavior of flow rate versus the angle. To evaluate pure effect of a single CNT bending on fluid flow rate, a new configuration is proposed and studied. The results showed that despite of CNT cross section experiencing no eccentricity, the flow rate decreases uniformly with increasing bending angle. Investigation of wall-fluid potential distribution in CNT cross section shows significant non-uniformity in bent cases. Future endeavors should be aimed at investigating similar effects for more complex fluids, clearly water is of great interest. Furthermore, investigation of effects associated to changing CNT length, diameter and inclination angle, as well as combination of them by pressure difference should be considered to complete the descriptive image.

References

- Ackerman, D.M., Skoulidas, A.I., Sholl, D.S. and Johnson, J.K. (2003), "Diffusivities of Ar and Ne in carbon nanotubes", *Mol. Simulat.*, **29**(10-11), 677-684.
<https://doi.org/10.1080/0892702031000103239>.
 Alexiadis, A. and Kassinos, S. (2008), "Influence of water model and nanotube rigidity on the density of water in carbon

- nanotubes”, *Chem. Eng. Sci.*, **63**(10), 2793-2797. <https://doi.org/10.1016/j.ces.2008.03.004>.
- Ang, E.Y.M., Ng, T.Y., Yeo, J., Liu, Z., Lin, R. and Geethalakshmi, K.R. (2019), “Effects of oscillating pressure on desalination performance of transverse flow CNT membrane”, *Desalination*, **451**, 35-44. <https://doi.org/10.1016/j.desal.2018.03.029>.
- Arash, B. and Wang, Q. (2014), “Molecular separation with carbon nanotubes”, *Comput. Mater. Sci.*, **90**, 50-55. <https://doi.org/10.1016/j.commatsci.2014.04.012>.
- Barclay, P. L. and Lukes, J. R. (2016), “Mass-flow-rate-controlled fluid flow in nanochannels by particle insertion and deletion”, *Phys. Rev. E*, **94**(6), 063303. <https://doi.org/10.1103/PhysRevE.94.063303>.
- Barzegar, H.R., Yan, A., Coh, S., Gracia-Espino, E., Ojeda-Aristizabal, C., Dunn, G., Zettl, A. (2017), “Spontaneous twisting of a collapsed carbon nanotube”, *Nano Res.*, **10**(6), 1942-1949. <https://doi.org/10.1007/s12274-016-1380-7>.
- Brenner, D.W. (1990), “Empirical potential for hydrocarbons for use in simulating the chemical vapor deposition of diamond films”, *Phys. Rev. B*, **42**(15), 9458-9471. <https://doi.org/10.1103/PhysRevB.42.9458>.
- Cannon, J. and Hess, O. (2010), “Fundamental dynamics of flow through carbon nanotube membranes”, *Microfluid. Nanofluid.*, **8**(1), 21-31. <https://doi.org/10.1007/s10404-009-0446-1>.
- Cao, B.Y., Chen, M. and Guo, Z.Y. (2006), “Liquid flow in surface-nanostructured channels studied by molecular dynamics simulation”, *Phys. Rev. E*, **74**(6), 066311. <https://doi.org/10.1103/PhysRevE.74.066311>.
- Chen, X., Cao, G., Han, A., Punyamurtula, V.K., Liu, L., Culligan, P.J., and Qiao, Y. (2008), “Nanoscale fluid transport: Size and rate effects”, *Nano Lett.*, **8**(9), 2988-2992. <https://doi.org/10.1021/nl802046b>.
- Chu, H., Zhang, Z., Liu, Y. and Leng, J. (2015), *Fillers and Reinforcements for Advanced Nanocomposites*, Woodhead Publishing, Cambridge, U.K.
- Derakhshan, S., Rezaee, M. and Sarrafha, H. (2015), “A molecular dynamics study of description models for shear viscosity in nanochannels: mixtures and effect of temperature”, *Nanoscale Microsc. Therm.*, **19**(3), 206-220. <https://doi.org/10.1080/15567265.2015.1065527>.
- Docherty, S.Y., Nicholls, W.D., Borg, M.K., Lockerby, D.A. and Reese, J.M. (2014), “Boundary conditions for molecular dynamics simulations of water transport through nanotubes”, *Proceedings of the Institution of Mechanical Engineers, Part C: Journal of Mechanical Engineering Science*, **228**(1), 186-195. <https://doi.org/10.1177/0954406213481760>.
- Feng, J., Chen, P., Zheng, D. and Zhong, W. (2018), “Transport diffusion in deformed carbon nanotubes”, *Physica A*, **493**, 155-161. <https://doi.org/10.1016/j.physa.2017.10.014>.
- He, J.X., Lu, H.J., Liu, Y., Wu, F.M., Nie, X.C., Zhou, X.Y. and Chen, Y.Y. (2012), “Asymmetry of the water flux induced by the deformation of a nanotube”, *Chinese Phys. B*, **21**(5), 054703. <https://doi.org/10.1088/1674-1056/21/5/054703>.
- Hoover, W.G. (1985), “Canonical dynamics: Equilibrium phase-space distributions”, *Phys. Rev. A*, **31**(3), 1695-1697. <https://doi.org/10.1103/PhysRevA.31.1695>.
- Huang, C., Nandakumar, K., Choi, P.Y.K. and Kostiuk, L.W. (2006), “Molecular dynamics simulation of a pressure-driven liquid transport process in a cylindrical nanopore using two self-adjusting plates”, *J. Chem. Phys.*, **124**(23), 234701. <https://doi.org/10.1063/1.2209236>.
- Hummer, G., Rasaiah, J. and Noworyta, J. (2001), “Water conduction through the hydrophobic channel of a carbon nanotube”, *Nature*, **414**(6860), 188. <https://doi.org/10.1038/35102535>.
- Iijima, S. (1991), “Helical microtubules of graphitic carbon”, *Nature*, **354**(6348), 56-58. <https://doi.org/10.1038/354056a0>.
- Kannam, S.K., Todd, B.D., Hansen, J.S. and Daivis, P.J. (2013), “How fast does water flow in carbon nanotubes?”, *J. Chem. Phys.*, **138**(9), 094701. <https://doi.org/10.1063/1.4793396>.
- Kaukonen, M., Gulans, A., Havu, P. and Kauppinen, E. (2012), “Lennard-Jones parameters for small diameter carbon nanotubes and water for molecular mechanics simulations from van der Waals density functional calculations”, *J. Comput. Chem.*, **33**(6), 652-658. <https://doi.org/10.1002/jcc.22884>.
- Köhler, M.H., Bordin, J.R., de Matos, C.F. and Barbosa, M.C. (2019), “Water in nanotubes: The surface effect”, *Chem. Eng. Sci.*, **203**, 54-67. <https://doi.org/10.1016/j.ces.2019.03.062>.
- Li, P., Wang, C., Zhang, Y. and Wei, F. (2014), “Air filtration in the free molecular flow regime: A review of high-efficiency particulate air filters based on Carbon Nanotubes”, *Small*, **10**, 4543-4561. <https://doi.org/10.1002/sml.201401553>.
- Li, S., Park, J.G., Liang, Z., Siegrist, T., Liu, T., Zhang, M., and Zhang, C. (2012), “In situ characterization of structural changes and the fraction of aligned carbon nanotube networks produced by stretching”, *Carbon*, **50**(10), 3859-3867. <https://doi.org/10.1016/j.carbon.2012.04.029>.
- Liakopoulos, A., Sofos, F. and Karakasidis, T.E. (2016), “Friction factor in nanochannel flows”, *Microfluid. Nanofluid.*, **20**(1), 1-7. <https://doi.org/10.1007/S10404-015-1699-5>.
- Liakopoulos, A., Sofos, F. and Karakasidis, T.E. (2017), “Darcy-Weisbach friction factor at the nanoscale: From atomistic calculations to continuum models”, *Phys. Fluids*, **29**(5), 052003. <https://doi.org/10.1063/1.4982667>.
- Lu, H., Li, J., Gong, X., Wan, R., Zeng, L. and Fang, H. (2008), “Water permeation and wavelike density distributions inside narrow nanochannels”, *Phys. Rev. B*, **77**(17), 174115. <https://doi.org/10.1103/PhysRevB.77.174115>.
- Madani, S.Y., Naderi, N., Dissanayake, O., Tan, A. and Seifalian, A.M. (2011), “A new era of cancer treatment: carbon nanotubes as drug delivery tools”, *Int. J. Nanomed.*, **6**, 2963-2979. <https://doi.org/10.2147/ijn.s16923>.
- Majumder, M., Chopra, N., Andrews, R. and Hinds, B.J. (2005), “Nanoscale hydrodynamics—enhanced flow in carbon nanotubes”, *Nature*, **438**(7064), 44. <https://doi.org/10.1038/43844a>.
- McGinnis, R.L., Reimund, K., Ren, J., Xia, L., Chowdhury, M.R., Sun, X., and Freeman, B. D. (2018), “Large-scale polymeric carbon nanotube membranes with sub-1.27-nm pores”, *Sci. Adv.*, **4**(3), 1700938. <https://doi.org/10.1126/sciadv.1700938>.
- Mendonça, B.H.S., de Freitas, D.N., Köhler, M.H., Batista, R.J.C., Barbosa, M.C. and de Oliveira, A.B. (2018), “Diffusion behavior of water confined in deformed carbon nanotubes”, *Physica A*, **517**, 491-498. <https://doi.org/10.1016/j.physa.2018.11.042>.
- Mendonça, B.H.S., Ternes, P., Salcedo, E., De Oliveira, A.B. and Barbosa, M.C. (2020), “Water diffusion in rough carbon nanotubes”, *J. Chem. Phys.*, **152**(2), 024708. <https://doi.org/10.1063/1.5129394>.
- Narang, J. (2019), “Multiwalled carbon nanotube wrapped nanoflake graphene composites for sensitive biosensing of leviteracetum”, *RSC Adv.*, **9**(33), 18814. <https://doi.org/10.1039/c9ra90046b>.
- Nosé, S. (1984), “A unified formulation of the constant temperature molecular dynamics methods”, *J. Chem. Phys.*, **81**(1), 511-519. <https://doi.org/10.1063/1.447334>.
- Panwar, N., Soehartono, A.M., Chan, K.K., Zeng, S., Xu, G., Qu, J., and Chen, X. (2019), “Nanocarbons for biology and medicine: Sensing, imaging, and drug delivery”, *Chemical Reviews*, **119**, 9559-9656. <https://doi.org/10.1021/acs.chemrev.9b00099>.
- Pérez-Sánchez, M. (2017), “Methodology for energy efficiency improvement analysis in pressurized irrigation networks. Practical application”, Ph.D. Dissertation, Universidad

- Politècnica de València, Spain.
- Razmkhah, M., Ahmadpour, A., Mosavian, M. T. H. and Moosavi, F. (2017), "What is the effect of carbon nanotube shape on desalination process? A simulation approach", *Desalination*, **407**, 103-115. <https://doi.org/10.1016/j.desal.2016.12.019>.
- Rezaee, M. and Ghassemi, H. (2020), "Anomalous behavior of fluid flow through thin carbon nanotubes", *Theor. Comp. Fluid Dyn.*, **34**(1-2), 177-186. <https://doi.org/10.1007/s00162-020-00521-3>.
- Ritos, K., Borg, M.K., Lockerby, D.A., Emerson, D.R. and Reese, J.M. (2015), "Hybrid molecular-continuum simulations of water flow through carbon nanotube membranes of realistic thickness", *Microfluid. Nanofluid.*, **19**(5), 997-1010. <https://doi.org/10.1007/s10404-015-1617-x>.
- Robinson, F., Shahbabaee, M. and Kim, D. (2019), "Deformation effect on water transport through nanotubes", *Energies*, **12**(23), 4424. <https://doi.org/10.3390/en12234424>.
- Shen, J. W., Kong, Z., Zhang, L. and Liang, L. (2016), "Controlled interval of aligned carbon nanotubes arrays for water desalination: A molecular dynamics simulation study", *Desalination*, **395**, 28-32. <https://doi.org/10.1016/j.desal.2016.05.024>.
- Shima, H. (2012), "Buckling of carbon nanotubes: A state of the art review", *Materials*, **5**(1), 47-84. <https://doi.org/10.3390/ma5010047>.
- Sofos, F., Karakasidis, T.E. and Liakopoulos, A. (2016), "Fluid structure and system dynamics in nanodevices for water desalination", *Desalin. Water Treat.*, **57**(25), 11561-11571. <https://doi.org/10.1080/19443994.2015.1049966>.
- Stukowski, A. (2010), "Visualization and analysis of atomistic simulation data with OVITO-the Open Visualization Tool", *Model. Simul. Mater. Sci.*, **18**(1), 015012. <https://doi.org/10.1088/0965-0393/18/1/015012>.
- Suga, K., Mori, Y., Moritani, R. and Kaneda, M. (2018), "Combined effects of molecular geometry and nanoconfinement on liquid flows through carbon nanotubes", *Phys. Rev. E*, **97**(5), 053109. <https://doi.org/10.1103/PhysRevE.97.053109>.
- Tersoff, J. (1988), "Empirical interatomic potential for carbon, with applications to amorphous carbon", *Phys. Rev. Lett.*, **61**(25), 2879-2882. <https://doi.org/10.1103/PhysRevLett.61.2879>.
- Wang, S., Liang, Z., Wang, B. and Zhang, C. (2006), "Statistical characterization of single-wall carbon nanotube length distribution", *Nanotechnology*, **17**(3), 634-639. <https://doi.org/10.1088/0957-4484/17/3/003>.
- Wang, Y., He, Z., Gupta, K.M., Shi, Q. and Lu, R. (2017), "Molecular dynamics study on water desalination through functionalized nanoporous graphene", *Carbon*, **116**, 120-127. <https://doi.org/10.1016/j.carbon.2017.01.099>.
- Wen, J., Zheng, D. and Zhong, W. (2015), "Shape-dependent collective diffusion coefficient of multi-layers graphene nanopores", *RSC Adv.*, **5**(120), 99573-99576. <https://doi.org/10.1039/C5RA21604D>.
- Wu, G., Tan, P., Wang, D., Li, Z., Peng, L., Hu, Y., and Chen, W. (2017), "High-performance supercapacitors based on electrochemical-induced vertical-aligned carbon nanotubes and polyaniline nanocomposite electrodes", *Sci. Rep.*, **7**(1), 1-8. <https://doi.org/10.1038/srep43676>.
- Yildiz, O. and Bradford, P.D. (2013), "Aligned carbon nanotube sheet high efficiency particulate air filters", *Carbon*, **64**, 295-304. <https://doi.org/10.1016/j.carbon.2013.07.066>.
- Yuan, D., Lin, W., Guo, R., Wong, C.P. and Das, S. (2012), "The fabrication of vertically aligned and periodically distributed carbon nanotube bundles and periodically porous carbon nanotube films through a combination of laser interference ablation and metal-catalyzed chemical vapor deposition", *Nanotechnology*, **23**(21), 215303. <https://doi.org/10.1088/0957-4484/23/21/215303>.
- Zhang, R. and Wei, F. (2019), "High-efficiency particulate air filters based on carbon nanotubes", *Nanotube Superfiber Mater.*, **2019**, 643-666. <https://doi.org/10.1016/B978-0-12-812667-7.00026-4>.
- Zhou, X., Wang, C., Wu, F., Feng, M., Li, J., Lu, H. and Zhou, R. (2013), "The ice-like water monolayer near the wall makes inner water shells diffuse faster inside a charged nanotube", *J. Chem. Phys.*, **138**(20), <https://doi.org/10.1063/1.4807383>.
- Zhou, X., Wu, F., Kou, J., Nie, X., Liu, Y. and Lu, H. (2013), "Vibrating-charge-driven water pump controlled by the deformation of the carbon nanotube", *J. Phys. Chem. B*, **117**(39), 11681-11686. <https://doi.org/10.1021/jp405036c>.

JL